

Supporting Information

A New Ru,Ru,Pt Supramolecular Architecture for Photocatalytic H₂ Production

Jessica Knoll White and Karen J. Brewer*

Department of Chemistry
Virginia Tech
Blacksburg, VA 24061 (USA)
E-mail: knoll.56@osu.edu

Table of Contents

Content	Page
Cover Page	1
Table of Contents	2
Experimental Section	3
Electrochemistry	6
Electronic Absorption Spectroscopy	8
Steady-State and Time-Resolved Emission Spectroscopy	10
Photocatalytic H ₂ Production	12
Three Dimensional Models	13
References	13

EXPERIMENTAL SECTION

Materials: All materials were used as received unless otherwise stated. The precursors *cis*-[PtCl₂(DMSO)₂], [(Ph₂phen)₂Ru(dpp)](PF₆)₂, and *cis,cis*-[(bpy)RuCl₂(DMSO)₂] and the ligand 2,3-bis(2-pyridyl)quinoxaline (dpq), were synthesized by previously reported methods.^[1] Ruthenium(III) trichloride trihydrate (RuCl₃•3H₂O), 2,2'-bipyridine (bpy), 4,7-diphenyl-1,10-phenanthroline (Ph₂phen), trifluoromethanesulfonic acid (HSO₃CF₃), silver trifluoromethanesulfonate (AgSO₃CF₃), lithium chloride (LiCl), and tetra-*n*-butylammonium chloride (Bu₄NCl) were purchased from Alfa Aesar. Sephadex® LH-20, *N,N*-dimethylaniline (DMA), and 2,3-bis(2-pyridyl)pyrazine (dpp) were received from Aldrich Chemical Company. Tetra-*n*-butylammonium hexafluorophosphate (Bu₄NPF₆) was purchased from Fluka. Ammonium hexafluorophosphate (NH₄PF₆) and tetrakis(dimethylsulfoxide)dichlororuthenium(II) (*cis*-[Ru(DMSO)₄Cl₂]) were purchased from Strem Chemicals, Inc. Ethanol (EtOH) was received from Decon Labs. Spectral grade acetonitrile (CH₃CN) was purchased from Burdick and Jackson. CH₃CN, toluene, diethyl ether (Et₂O), ethylene glycol, and 80-200 mesh alumina were purchased from Fisher Scientific.

Synthesis:

[(Ph₂phen)₂Ru(dpp)RuCl₂(bpy)](PF₆)₂ was synthesized by heating at reflux [(Ph₂phen)₂Ru(dpp)](PF₆)₂ (0.30 g, 0.39 mmol) and excess *cis,cis*-[(bpy)RuCl₂(DMSO)₂] (0.39 g, 0.80 mmol) in 40 mL of EtOH for 16 h. The reaction mixture was cooled to RT followed by addition of 0.5 g of NH₄PF₆. The precipitate was collected by vacuum filtration and washed with 100 mL of H₂O. Purification was achieved by Sephadex® LH-20 size exclusion chromatography (2.2 cm x 100 cm) utilizing a 2:1 EtOH/CH₃CN mobile phase. The green-brown product that eluted first was collected and the solvent was removed under vacuum. The product was dissolved in minimal CH₃CN (5 mL) and added dropwise to 300 mL of Et₂O by syringe filtration. The green-brown precipitate was collected by vacuum filtration, washed with 60 mL of Et₂O and dried under vacuum (0.29 g, 0.18 mmol, yield = 45 %). (+)ESI-MS: [M-PF₆]⁺, *m/z* = 1473.14, [M-2PF₆]²⁺, *m/z* = 664.09.

[(Ph₂phen)₂Ru(dpp)Ru(bpy)(dpp)](PF₆)₄ was synthesized by heating at reflux [(Ph₂phen)₂Ru(dpp)RuCl₂(bpy)](PF₆)₂ (0.30 g, 0.19 mmol) and two equivalents of AgSO₃CF₃ (0.97 g, 0.38 mmol) in 30 mL of EtOH for 2 h to remove Cl⁻ ligands. The hot reaction mixture was then added to a hot, stirring solution of dpp (0.3 g, 1.2 mmol) in 20 mL of ethylene glycol and the mixture was heated at reflux for 16 h. The reaction mixture was then cooled to RT and 0.075 g of Bu₄NCl was added and stirred for 30 minutes to precipitate Ag⁺ as AgCl. Excess NH₄PF₆ (0.5 g) was added and the precipitate was collected by vacuum filtration and washed with 50 mL of H₂O. Purification was achieved by Sephadex® LH-20 size exclusion chromatography (2.2 cm x 100 cm) with a 2:1 EtOH/CH₃CN mobile phase. The red-purple product that eluted first was collected and the solvent was removed under vacuum. The product was dissolved in minimal CH₃CN (5 mL) and added dropwise to 300 mL of Et₂O by syringe filtration. The red precipitate was collected by vacuum filtration, washed with 60 mL of Et₂O, and dried under vacuum (0.23 g, 0.11 mmol, yield = 60 %). (+)ESI-MS: [M-PF₆]⁺, *m/z* = 1927.21, [M-2PF₆]²⁺, *m/z* = 890.73, [M-3PF₆]³⁺, *m/z* = 545.76.

[(Ph₂phen)₂Ru(dpp)Ru(bpy)(dpq)](PF₆)₄ was synthesized and purified following the procedure used for [(Ph₂phen)₂Ru(dpp)Ru(bpy)(dpp)](PF₆)₄ by substituting dpq (0.33 g, 1.2 mmol) in the second step, producing a dark purple-red color precipitate (0.21 g, 0.10 mmol, yield = 55 %). (+)ESI-MS: [M-2PF₆]²⁺, *m/z* = 890.73.

[(Ph₂phen)₂Ru(dpp)Ru(bpy)(dpp)PtCl₂](PF₆)₄ was synthesized by heating at reflux a mixture of [(Ph₂phen)₂Ru(dpp)Ru(bpy)(dpp)](PF₆)₄ (0.10 g, 0.048 mmol) and excess *cis*-[PtCl₂(DMSO)₂] (0.10 g, 0.24 mmol) in 30 mL EtOH for 4 h. The reaction mixture was cooled to RT and 0.5 g of NH₄PF₆ was added. The precipitate was collected by vacuum filtration and washed with 60 mL of H₂O. The product

was dissolved in minimal CH₃CN (5 mL) and added dropwise to 300 mL of Et₂O by syringe filtration to remove Pt⁰ particles. The red precipitate was collected by vacuum filtration, washed with 50 mL of Et₂O and dried under vacuum (0.11 g, 0.046 mmol, yield = 95 %). (+)ESI-MS: [M–PF₆]⁺, *m/z* = 2193.11, [M–2PF₆]²⁺, *m/z* = 1024.07, [M–3PF₆]³⁺, *m/z* = 634.07.

[(Ph₂phen)₂Ru(dpp)Ru(bpy)(dpq)PtCl₂](PF₆)₄ was synthesized and purified following the procedure used for [(Ph₂phen)₂Ru(dpp)Ru(bpy)(dpp)PtCl₂](PF₆)₄ by substituting [(Ph₂phen)₂Ru(dpp)Ru(bpy)(dpq)](PF₆)₄ (0.10 g, 0.047 mmol), producing a dark purple-red precipitate (0.11 g, 0.045 mmol, yield = 95 %). (+)ESI-MS: [M–2PF₆]²⁺, *m/z* = 1049.08, [M–3PF₆]³⁺, *m/z* = 651.07.

Mass spectrometry: Positive ion electrospray ionization mass spectrometry, (+)ESI-MS, experiments were performed using an Agilent Technologies 6220 Accurate-Mass time-of-flight (TOF) instrument with a dual ESI source. Samples were dissolved in HPLC grade CH₃CN. Isotopic distribution patterns were simulated with Sheffield Chemputer^[21] (REF) and compared to the observed molecular ion peaks.

Electrochemistry: Cyclic voltammetry (CV) and square wave voltammetry (SWV) were performed with an Epsilon potentiostat from Bioanalytical Systems, Inc. using a one compartment, three electrode cell with a glassy carbon working electrode, silver wire pseudo reference electrode, and a platinum wire auxiliary electrode. Ferrocene was added to the sample as an internal standard (FeCp₂⁺/FeCp₂ = 0.46 V vs. Ag/AgCl(3 M NaCl)) following electrochemical analysis. The working electrode was polished with 0.5 μm alumina paste prior to each experiment. The metal complex was dissolved in an CH₃CN electrolyte solution containing 0.1 M Bu₄NPF₆ which was deoxygenated by bubbling with Ar for 10 minutes. CV studies were performed at a scan rate of 0.1 V/s. SWV studies were performed with pulse frequency (τ) = 15 Hz, pulse time (t_p) = 30 ms, fixed pulse potential magnitude (ΔE_p) = 25 mV, and potential step (ΔE_s) = 4 mV.

Electronic absorption spectroscopy: Electronic absorption spectra were collected using an Agilent 8453 diode array UV-Vis spectrophotometer with a spectral range of 190 to 1100 nm and 1 nm resolution. Samples were dissolved in RT spectral grade CH₃CN and measured in a 1 cm or 0.2 cm quartz cuvette (Starna Cells, Inc.; Atascadero, CA, USA). Extinction coefficient experiments were performed in triplicate. Solutions were prepared gravimetrically.

Steady-state and time-resolved emission spectroscopy: Steady-state emission was measured using a QuantaMaster Model QM-200-45E fluorimeter (Figure 2.4A) from Photon Technologies International, Inc. The excitation source was a 150 W Xe arc lamp that was cooled by water circulation. The emission was collected at a 90° angle with a thermoelectrically cooled Hamamatsu 1527 photomultiplier tube (PMT) in photon counting mode with a 0.25 nm resolution. The monochromator used Czerny-Turner style grating set to 1200 lines/mm and 750 nm blaze. The slit widths for the excitation and emission monochromators were adjusted to 1.5 mm (± 6 nm). The sample was dissolved in RT spectral grade CH₃CN with an absorbance ca. 0.3 at the chosen excitation wavelength. The solutions were deoxygenated by bubbling with Ar for 10 minutes prior to analysis. Recorded spectra were an average of three scans unless otherwise stated. The quantum yields of emission (Φ^{em}) were calculated using [Os(bpy)₃](PF₆)₂ as a standard (Φ^{em} = 0.0046 in RT deoxygenated CH₃CN).^[3] 77 K emission spectra were obtained by dissolving the sample in 4:1 EtOH/MeOH in an NMR tube and slowly immersing the sample in a liquid N₂ finger dewar. All emission spectra were corrected for PMT response. Time-resolved emission spectroscopy measurements were performed using a Photon Technologies International, Inc. PL-2300 N₂ laser with a PL-201 tunable dye laser. An emission monochromator was set to the maximum emission wavelength determined by steady-state emission measurements. A Hamamatsu R928 PMT operating in direct analog mode collected the time profile at a 90° angle relative to the excitation source. The signal was displayed on a LeCroy 9361 Dual 300 MHz oscilloscope (2.5 Gs/s). The data were applied to an exponential decay function, **Equation S1**,

$$I(t) = \sum_i \alpha_i e^{-\frac{t}{\tau_i}} \quad (\text{S1})$$

where $I(t)$ is the intensity of the signal at time t after the laser pulse, $\sum_i \alpha_i$ is the sum of the fractions that are contributed by each component to the overall observed decay, i is the component, and τ_i is the excited state lifetime of each component. The signals measured as potential (V) were graphed versus time, and a plot of $\ln(V)$ versus time yields a straight line with a slope that corresponds to τ^{-1} . The solutions were deoxygenated by bubbling with Ar for 10 minutes prior to analysis.

Photocatalytic H₂ production: H₂ production experiments were performed using a locally designed LED array.^[4] The light sources were blue Luxeon® V Star LEDs with a spectral coverage of 470 ± 10 nm. The chemical actinometer K₃[Fe(C₂O₄)₃] (potassium ferrioxalate) was used to determine the light flux of the LEDs. The calculated flux of $2.3 \pm 0.1 \times 10^{19}$ photons/min was the average of three experiments. HY-OPTIMA™ 700 in-line process H₂ sensors from H2scan (Valencia, CA) were used to quantify H₂ production in real time. The sensors were calibrated periodically to ensure accurate H₂ readings. Glass photolysis reaction cells were designed and manufactured locally. The septum-capped cells were tightly attached to the H₂ sensor, and air was removed from the system with an Ar flow for 30 minutes. The metal complex stock solution in spectral grade CH₃CN and H₂O acidified to pH 2 with HSO₃CF₃ were injected into the reaction cells. The solution was deoxygenated by bubbling with Ar for 15 minutes. DMA was deoxygenated separately and injected into the cell immediately prior to photolysis. The total volume of the solution was 4.5 mL, and the headspace volume was 15.3 mL. The LEDs were turned on to begin photolysis directly after injection of DMA. The evolution of H₂ was monitored in real time using MOXA Pcomm Lite terminal emulator software. The % H₂ output was converted to moles of H₂, and the TON (turnover number) of the catalyst was calculated using **Equation S2**.

$$TON = \frac{\text{moles of } H_2 \text{ produced}}{\text{moles of catalyst}} \quad (\text{S2})$$

The quantum yield of H₂ production at time t was calculated using **Equation S3**.

$$\Phi_{H_2}(t) = \frac{\text{moles of } H_2 \text{ produced}}{\text{moles of incident photons}} \times 2 \quad (\text{S3})$$

The moles of incident photons were calculated using the light flux. The ratio of moles of H₂ produced and the moles of incident photons was multiplied by two due to the need for two photons to produce one H₂ molecule. Experiments were performed in triplicate.

ELECTROCHEMISTRY

Table S1. Electrochemical Data for the [(Ph₂phen)₂Ru(dpp)RuCl₂(bpy)](PF₆)₂, [(Ph₂phen)₂Ru(dpp)Ru(bpy)(BL)](PF₆)₄, [(Ph₂phen)₂Ru(dpp)Ru(bpy)(BL)PtCl₂](PF₆)₄, [(Ph₂phen)₂Ru(dpp)]₂RuCl₂(PF₆)₄, [{(Ph₂phen)₂Ru(dpp)}₂Ru(BL)](PF₆)₆, and [{(Ph₂phen)₂Ru(dpp)}₂Ru(BL)PtCl₂](PF₆)₆ Complexes^a

Complex	E _{1/2} (V vs. Ag/AgCl)		
	Oxidation (assignment) ^b		Reduction (assignment) ^c
[(Ph ₂ phen) ₂ Ru (dpp)RuCl ₂ (bpy)](PF ₆) ₂	0.66 (Ru ^{II/III})	1.58 (Ru ^{II/III})	-0.80 (dpp ^{0/-})
[(Ph ₂ phen) ₂ Ru (dpp)Ru(bpy)(dpp)](PF ₆) ₄	1.53 (Ru ^{II/III})		-0.54 (dpp ^{0/-}) -1.00 (dpp ^{0/-})
[(Ph ₂ phen) ₂ Ru (dpp)Ru(bpy)(dpq)](PF ₆) ₄	1.54 (Ru ^{II/III})		-0.49 (dpp ^{0/-}) -0.77 (dpq ^{0/-})
[(Ph ₂ phen) ₂ Ru (dpp)Ru(bpy)(dpp)PtCl ₂](PF ₆) ₄	1.54 (Ru ^{II/III})		-0.39 (dpp ^{0/-}) -0.60 (dpp ^{0/-})
[(Ph ₂ phen) ₂ Ru (dpp)Ru(bpy)(dpq)PtCl ₂](PF ₆) ₄	1.55 (Ru ^{II/III})		-0.08 (dpq ^{0/-}) -0.60 (dpp ^{0/-})
[{(Ph ₂ phen) ₂ Ru (dpp)} ₂ RuCl ₂](PF ₆) ₄	0.86 (Ru ^{II/III})	1.59 (2 Ru ^{II/III})	-0.68 (dpp ^{0/-}) -0.81 (dpp ^{0/-})
[{(Ph ₂ phen) ₂ Ru (dpp)} ₂ Ru(dpp)](PF ₆) ₆	1.55 (2 Ru ^{II/III})		-0.45 (dpp ^{0/-}) -0.60 (dpp ^{0/-}) -1.02 (dpp ^{0/-})
[{(Ph ₂ phen) ₂ Ru (dpp)} ₂ Ru(dpq)](PF ₆) ₆	1.55 (2 Ru ^{II/III})		-0.42 (dpp ^{0/-}) -0.58 (dpp ^{0/-}) -0.79 (dpq ^{0/-})
[{(Ph ₂ phen) ₂ Ru (dpp)} ₂ Ru(dpp)PtCl ₂](PF ₆) ₆	1.56 (2 Ru ^{II/III})		-0.33 (dpp ^{0/-}) -0.53 (dpp ^{0/-}) -0.64 (dpp ^{0/-})
[{(Ph ₂ phen) ₂ Ru (dpp)} ₂ Ru(dpq)PtCl ₂](PF ₆) ₆	1.57 (2 Ru ^{II/III})		-0.02 (dpq ^{0/-}) -0.50 (dpp ^{0/-}) -0.65 (dpp ^{0/-})

^a Measurements recorded in deoxygenated CH₃CN at RT with 0.1 M Bu₄NPF₆ electrolyte. Ph₂phen = 4,7-diphenyl-1,10-phenanthroline, bpy = 2,2'-bipyridine, dpp = 2,3-bis(2-pyridyl)pyrazine, dpq = 2,3-bis(2-pyridyl)quinoxaline. Potentiostat resolution is ± 10 mV. ^b Bold indicates terminal Ru. ^c Bold indicates BL.

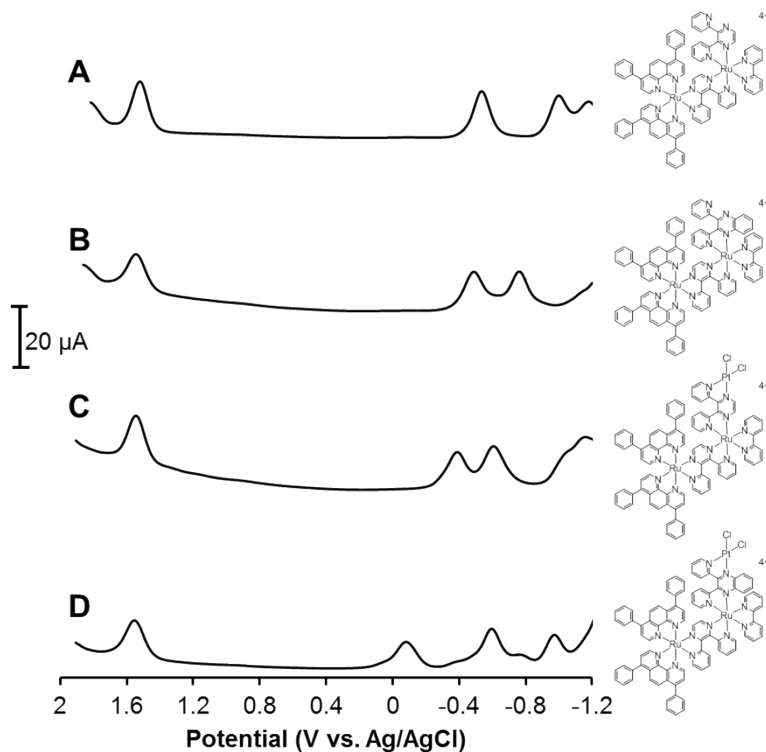


Figure S1. Square wave voltammograms of A) $[(\text{Ph}_2\text{phen})_2\text{Ru}(\text{dpp})\text{Ru}(\text{bpy})(\text{dpp})](\text{PF}_6)_4$, B) $[(\text{Ph}_2\text{phen})_2\text{Ru}(\text{dpp})\text{Ru}(\text{bpy})(\text{dpq})](\text{PF}_6)_4$, C) $[(\text{Ph}_2\text{phen})_2\text{Ru}(\text{dpp})\text{Ru}(\text{bpy})(\text{dpp})\text{PtCl}_2](\text{PF}_6)_4$, and D) $[(\text{Ph}_2\text{phen})_2\text{Ru}(\text{dpp})\text{Ru}(\text{bpy})(\text{dpq})\text{PtCl}_2](\text{PF}_6)_4$ measured in deoxygenated RT CH_3CN with 0.1 M Bu_4NPF_6 supporting electrolyte in a one compartment, three electrode cell with a glassy carbon working electrode, Ag/AgCl reference electrode, and a platinum wire auxiliary electrode.

ELECTRONIC ABSORPTION SPECTROSCOPY

Table S2. Electronic Absorption Spectroscopic Data for the $[(\text{Ph}_2\text{phen})_2\text{Ru}(\text{dpp})\text{RuCl}_2(\text{bpy})](\text{PF}_6)_2$, $[(\text{Ph}_2\text{phen})_2\text{Ru}(\text{dpp})\text{Ru}(\text{bpy})(\text{BL})](\text{PF}_6)_4$, $[(\text{Ph}_2\text{phen})_2\text{Ru}(\text{dpp})\text{Ru}(\text{bpy})(\text{BL})\text{PtCl}_2](\text{PF}_6)_4$, $[\{(\text{Ph}_2\text{phen})_2\text{Ru}(\text{dpp})\}_2\text{RuCl}_2](\text{PF}_6)_4$, $[\{(\text{Ph}_2\text{phen})_2\text{Ru}(\text{dpp})\}_2\text{Ru}(\text{BL})](\text{PF}_6)_6$, and $[\{(\text{Ph}_2\text{phen})_2\text{Ru}(\text{dpp})\}_2\text{Ru}(\text{BL})\text{PtCl}_2](\text{PF}_6)_6$ Complexes ^a

Complex	$\lambda_{\text{max}}^{\text{abs}}$ (nm)	$\epsilon \times 10^{-4}$ ($\text{M}^{-1}\text{cm}^{-1}$)	Assignment
$[(\text{Ph}_2\text{phen})_2\text{Ru}(\text{dpp})\text{RuCl}_2(\text{bpy})](\text{PF}_6)_2$	278	11	$\text{Ph}_2\text{phen } \pi \rightarrow \pi^*$, $\text{bpy } \pi \rightarrow \pi^*$
	326 (sh)	3.7	$\text{dpp } \pi \rightarrow \pi^*$
	450	2.2	$\text{Ru}(\text{d}\pi) \rightarrow \text{Ph}_2\text{phen}(\pi^*)$ CT, $\text{Ru}(\text{d}\pi) \rightarrow \text{bpy}(\pi^*)$ CT
	580	1.9	$\text{Ru}(\text{d}\pi) \rightarrow \text{dpp}(\pi^*)$ CT
$[(\text{Ph}_2\text{phen})_2\text{Ru}(\text{dpp})\text{Ru}(\text{bpy})(\text{dpp})](\text{PF}_6)_4$	278	14	$\text{Ph}_2\text{phen } \pi \rightarrow \pi^*$, $\text{bpy } \pi \rightarrow \pi^*$
	322 (sh)	5.8	$\text{dpp } \pi \rightarrow \pi^*$
	436	3.0	$\text{Ru}(\text{d}\pi) \rightarrow \text{Ph}_2\text{phen}(\pi^*)$ CT, $\text{Ru}(\text{d}\pi) \rightarrow \text{bpy}(\pi^*)$ CT
	535	2.8	$\text{Ru}(\text{d}\pi) \rightarrow \text{dpp}(\pi^*)$ CT
$[(\text{Ph}_2\text{phen})_2\text{Ru}(\text{dpp})\text{Ru}(\text{bpy})(\text{dpq})](\text{PF}_6)_4$	278	14	$\text{Ph}_2\text{phen } \pi \rightarrow \pi^*$, $\text{bpy } \pi \rightarrow \pi^*$
	328 (sh)	4.8	$\text{dpp } \pi \rightarrow \pi^*$, $\text{dpq } \pi \rightarrow \pi^*$
	436	2.4	$\text{Ru}(\text{d}\pi) \rightarrow \text{Ph}_2\text{phen}(\pi^*)$ CT, $\text{Ru}(\text{d}\pi) \rightarrow \text{bpy}(\pi^*)$ CT
	545	2.3	$\text{Ru}(\text{d}\pi) \rightarrow \text{dpp}(\pi^*)$ CT, $\text{Ru}(\text{d}\pi) \rightarrow \text{dpq}(\pi^*)$ CT
$[(\text{Ph}_2\text{phen})_2\text{Ru}(\text{dpp})\text{Ru}(\text{bpy})(\text{dpp})\text{PtCl}_2](\text{PF}_6)_4$	277	11	$\text{Ph}_2\text{phen } \pi \rightarrow \pi^*$, $\text{bpy } \pi \rightarrow \pi^*$
	323 (sh)	5.6	$\text{dpp } \pi \rightarrow \pi^*$
	434	2.8	$\text{Ru}(\text{d}\pi) \rightarrow \text{Ph}_2\text{phen}(\pi^*)$ CT, $\text{Ru}(\text{d}\pi) \rightarrow \text{bpy}(\pi^*)$ CT
	542	2.9	$\text{Ru}(\text{d}\pi) \rightarrow \text{dpp}(\pi^*)$ CT
$[(\text{Ph}_2\text{phen})_2\text{Ru}(\text{dpp})\text{Ru}(\text{bpy})(\text{dpq})\text{PtCl}_2](\text{PF}_6)_4$	277	12	$\text{Ph}_2\text{phen } \pi \rightarrow \pi^*$, $\text{bpy } \pi \rightarrow \pi^*$
	326 (sh)	5.1	$\text{dpp } \pi \rightarrow \pi^*$, $\text{dpq } \pi \rightarrow \pi^*$
	434	2.4	$\text{Ru}(\text{d}\pi) \rightarrow \text{Ph}_2\text{phen}(\pi^*)$ CT, $\text{Ru}(\text{d}\pi) \rightarrow \text{bpy}(\pi^*)$ CT
	543	2.2	$\text{Ru}(\text{d}\pi) \rightarrow \text{dpp}(\pi^*)$ CT, $\text{Ru}(\text{d}\pi) \rightarrow \text{dpq}(\pi^*)$ CT
$[\{(\text{Ph}_2\text{phen})_2\text{Ru}(\text{dpp})\}_2\text{RuCl}_2](\text{PF}_6)_4$	276	21	$\text{Ph}_2\text{phen } \pi \rightarrow \pi^*$
	315 (sh)	9.1	$\text{dpp } \pi \rightarrow \pi^*$
	442	4.5	$\text{Ru}(\text{d}\pi) \rightarrow \text{Ph}_2\text{phen}(\pi^*)$ CT
	625	3.4	$\text{Ru}(\text{d}\pi) \rightarrow \text{dpp}(\pi^*)$ CT
$[\{(\text{Ph}_2\text{phen})_2\text{Ru}(\text{dpp})\}_2\text{Ru}(\text{dpp})](\text{PF}_6)_6$	276	20	$\text{Ph}_2\text{phen } \pi \rightarrow \pi^*$
	340 (sh)	5.7	$\text{dpp } \pi \rightarrow \pi^*$
	432	4.2	$\text{Ru}(\text{d}\pi) \rightarrow \text{Ph}_2\text{phen}(\pi^*)$ CT
	554	4.2	$\text{Ru}(\text{d}\pi) \rightarrow \text{dpp}(\pi^*)$ CT
$[\{(\text{Ph}_2\text{phen})_2\text{Ru}(\text{dpp})\}_2\text{Ru}(\text{dpq})](\text{PF}_6)_6$	276	14	$\text{Ph}_2\text{phen } \pi \rightarrow \pi^*$
	340 (sh)	5.5	$\text{dpp } \pi \rightarrow \pi^*$, $\text{dpq } \pi \rightarrow \pi^*$
	430	3.6	$\text{Ru}(\text{d}\pi) \rightarrow \text{Ph}_2\text{phen}(\pi^*)$ CT
	550	3.6	$\text{Ru}(\text{d}\pi) \rightarrow \text{dpp}(\pi^*)$ CT, $\text{Ru}(\text{d}\pi) \rightarrow \text{dpq}(\pi^*)$ CT
$[\{(\text{Ph}_2\text{phen})_2\text{Ru}(\text{dpp})\}_2\text{Ru}(\text{dpp})\text{PtCl}_2](\text{PF}_6)_6$	276	17	$\text{Ph}_2\text{phen } \pi \rightarrow \pi^*$
	326 (sh)	7.7	$\text{dpp } \pi \rightarrow \pi^*$
	432	4.2	$\text{Ru}(\text{d}\pi) \rightarrow \text{Ph}_2\text{phen}(\pi^*)$ CT
	550	4.2	$\text{Ru}(\text{d}\pi) \rightarrow \text{dpp}(\pi^*)$ CT
$[\{(\text{Ph}_2\text{phen})_2\text{Ru}(\text{dpp})\}_2\text{Ru}(\text{dpq})\text{PtCl}_2](\text{PF}_6)_6$	276	14	$\text{Ph}_2\text{phen } \pi \rightarrow \pi^*$
	340 (sh)	5.2	$\text{dpp } \pi \rightarrow \pi^*$, $\text{dpq } \pi \rightarrow \pi^*$
	430	3.6	$\text{Ru}(\text{d}\pi) \rightarrow \text{Ph}_2\text{phen}(\pi^*)$ CT
	550	3.1	$\text{Ru}(\text{d}\pi) \rightarrow \text{dpp}(\pi^*)$ CT, $\text{Ru}(\text{d}\pi) \rightarrow \text{dpq}(\pi^*)$ CT

^a Measurements recorded in spectral grade CH_3CN at RT in a 1 cm quartz cuvette. Ph_2phen = 4,7-diphenyl-1,10-phenanthroline, bpy = 2,2'-bipyridine, dpp = 2,3-bis(2-pyridyl)pyrazine, dpq = 2,3-bis(2-pyridyl)quinoxaline. Extinction coefficient values were determined from the average of three experiments.

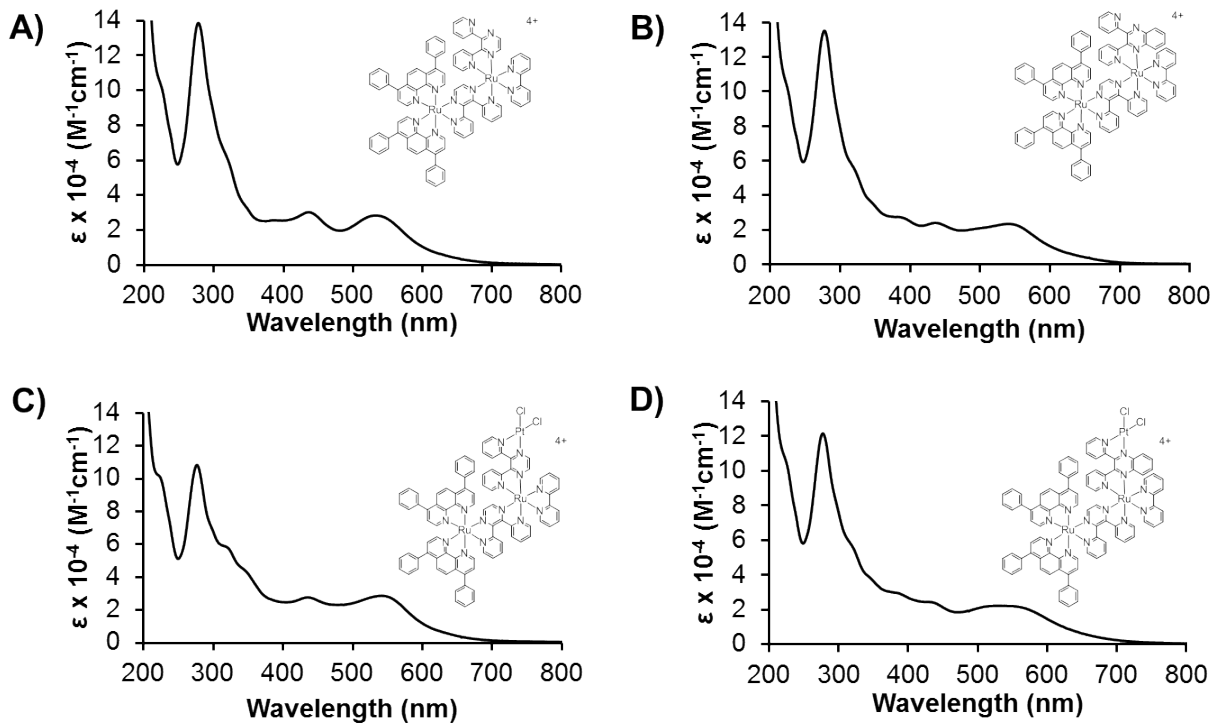


Figure S2. Electronic absorption spectra of A) $[(\text{Ph}_2\text{phen})_2\text{Ru}(\text{dpp})\text{Ru}(\text{bpy})(\text{dpp})](\text{PF}_6)_4$, B) $[(\text{Ph}_2\text{phen})_2\text{Ru}(\text{dpp})\text{Ru}(\text{bpy})(\text{dpq})](\text{PF}_6)_4$, C) $[(\text{Ph}_2\text{phen})_2\text{Ru}(\text{dpp})\text{Ru}(\text{bpy})(\text{dpp})\text{PtCl}_2](\text{PF}_6)_4$, and D) $[(\text{Ph}_2\text{phen})_2\text{Ru}(\text{dpp})\text{Ru}(\text{bpy})(\text{dpq})\text{PtCl}_2](\text{PF}_6)_4$ measured in RT CH_3CN .

EMISSION SPECTROSCOPY

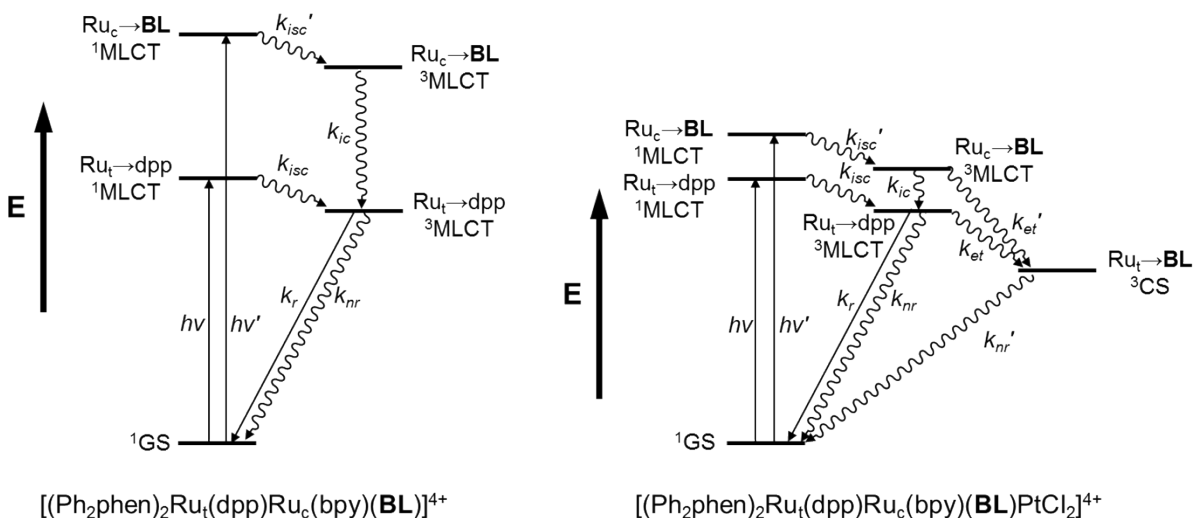


Figure S3. Simplified state diagrams for $[(\text{Ph}_2\text{phen})_2\text{Ru}(\text{dpp})\text{Ru}(\text{bpy})(\text{BL})](\text{PF}_6)_4$ and $[(\text{Ph}_2\text{phen})_2\text{Ru}(\text{dpp})\text{Ru}(\text{bpy})(\text{BL})\text{PtCl}_2](\text{PF}_6)_4$. BL = dpp = 2,3-bis(2-pyridyl)pyrazine or dpq = 2,3-bis(2-pyridyl)quinoxaline, Ph_2phen = 4,7-diphenyl-1,10-phenanthroline, bpy = 2,2'-bipyridine, $^1\text{MLCT}$ = singlet metal-to-ligand charge transfer, $^3\text{MLCT}$ = triplet metal-to-ligand charge transfer, ^3CS = triplet charge separated state, k_r = rate constant for radiative decay, k_{nr} = rate constant for non-radiative decay, k_{isc} = rate constant for intersystem crossing, k_{ic} = rate constant for internal conversion, k_{et} = rate constant for electron transfer.

Table S3. Steady-State and Time-Resolved Emission Spectroscopy Data for the $[(\text{Ph}_2\text{phen})_2\text{Ru}(\text{dpp})\text{Ru}(\text{bpy})(\text{BL})](\text{PF}_6)_4$, $[(\text{Ph}_2\text{phen})_2\text{Ru}(\text{dpp})\text{Ru}(\text{bpy})(\text{BL})\text{PtCl}_2](\text{PF}_6)_4$, $[\{(\text{Ph}_2\text{phen})_2\text{Ru}(\text{dpp})\}_2\text{Ru}(\text{BL})](\text{PF}_6)_6$, and $[\{(\text{Ph}_2\text{phen})_2\text{Ru}(\text{dpp})\}_2\text{Ru}(\text{BL})\text{PtCl}_2](\text{PF}_6)_6$ Complexes ^a

Complex	λ^{em} (nm)	$\Phi^{\text{em}} \times 10^3$	τ (μs)	λ^{em} (nm)
	RT	RT	RT	77 K ^b
$[(\text{Ph}_2\text{phen})_2\text{Ru}(\text{dpp})\text{Ru}(\text{bpy})(\text{dpp})](\text{PF}_6)_4$	762	1.5	0.12	695
$[(\text{Ph}_2\text{phen})_2\text{Ru}(\text{dpp})\text{Ru}(\text{bpy})(\text{dpq})](\text{PF}_6)_4$	762	1.5	0.12	706
$[(\text{Ph}_2\text{phen})_2\text{Ru}(\text{dpp})\text{Ru}(\text{bpy})(\text{dpp})\text{PtCl}_2](\text{PF}_6)_4$	765	1.1	0.090	705
$[(\text{Ph}_2\text{phen})_2\text{Ru}(\text{dpp})\text{Ru}(\text{bpy})(\text{dpq})\text{PtCl}_2](\text{PF}_6)_4$	761	0.52	0.10	706
$[\{(\text{Ph}_2\text{phen})_2\text{Ru}(\text{dpp})\}_2\text{Ru}(\text{dpp})](\text{PF}_6)_6$	764	1.0	0.11	705
$[\{(\text{Ph}_2\text{phen})_2\text{Ru}(\text{dpp})\}_2\text{Ru}(\text{dpq})](\text{PF}_6)_6$	764	1.1	0.11	715
$[\{(\text{Ph}_2\text{phen})_2\text{Ru}(\text{dpp})\}_2\text{Ru}(\text{dpp})\text{PtCl}_2](\text{PF}_6)_6$	766	0.71	0.077	705
$[\{(\text{Ph}_2\text{phen})_2\text{Ru}(\text{dpp})\}_2\text{Ru}(\text{dpq})\text{PtCl}_2](\text{PF}_6)_6$	760	0.37	0.075	715

^a RT measurements were performed on CH_3CN solutions deoxygenated with Ar and excited at 540 nm. Values corrected for PMT response. Ph_2phen = 4,7-diphenyl-1,10-phenanthroline, bpy = 2,2'-bipyridine, dpp = 2,3-bis(2-pyridyl)pyrazine, dpq = 2,3-bis(2-pyridyl)quinoxaline. ^b 77 K measurements were performed with complexes in a 4:1 (v/v) EtOH/MeOH glass and excited at 540 nm.

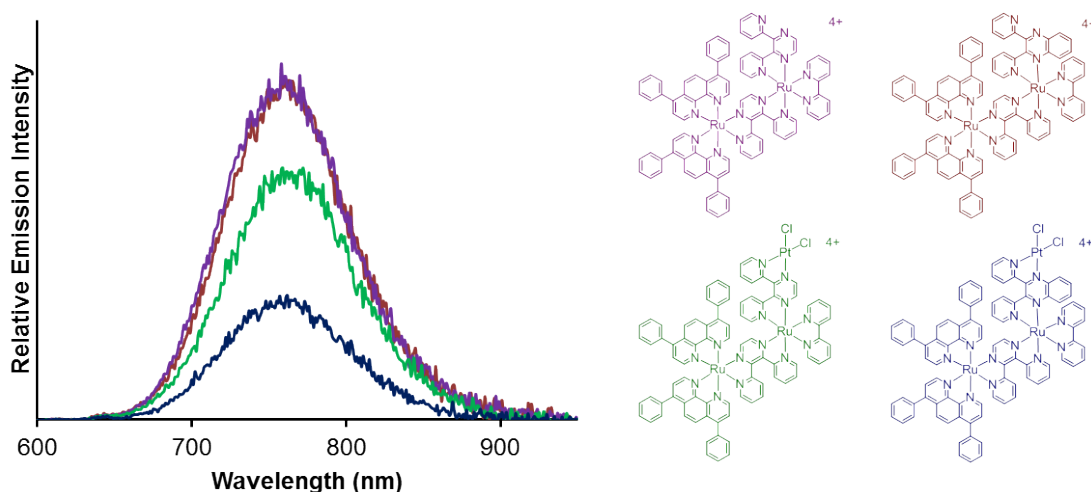


Figure S4. Relative steady-state emission spectra of $[(\text{Ph}_2\text{phen})_2\text{Ru}(\text{dpp})\text{Ru}(\text{bpy})(\text{dpp})](\text{PF}_6)_4$ (purple), $[(\text{Ph}_2\text{phen})_2\text{Ru}(\text{dpp})\text{Ru}(\text{bpy})(\text{dpq})](\text{PF}_6)_4$ (maroon), $[(\text{Ph}_2\text{phen})_2\text{Ru}(\text{dpp})\text{Ru}(\text{bpy})(\text{dpp})\text{PtCl}_2](\text{PF}_6)_4$ (green), and $[(\text{Ph}_2\text{phen})_2\text{Ru}(\text{dpp})\text{Ru}(\text{bpy})(\text{dpq})\text{PtCl}_2](\text{PF}_6)_4$ (blue) measured in deoxygenated RT CH_3CN with $\lambda^{\text{exc}} = 540$ nm. Spectra were corrected for PMT response.

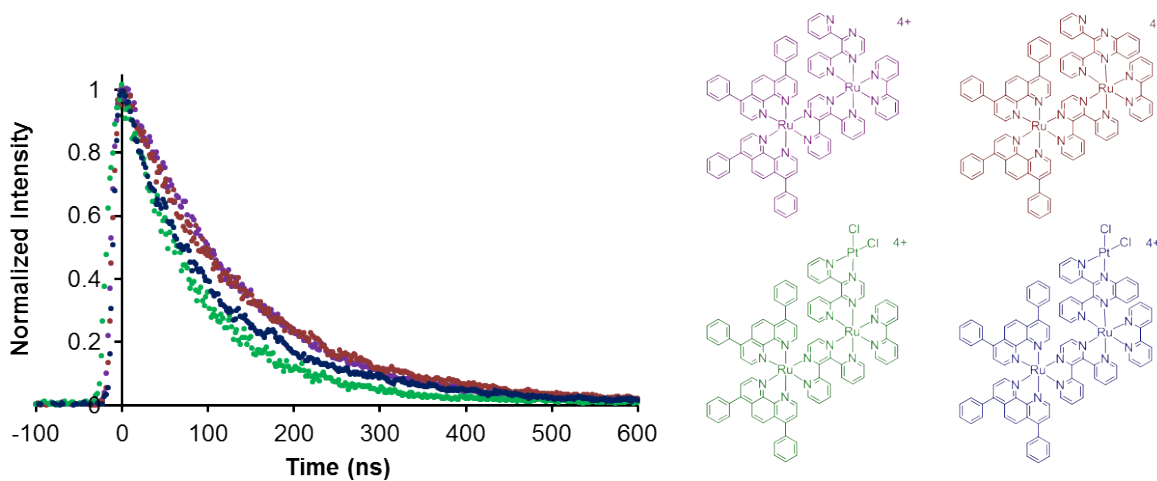


Figure S5. Normalized emission decay curves of $[(\text{Ph}_2\text{phen})_2\text{Ru}(\text{dpp})\text{Ru}(\text{bpy})(\text{dpp})](\text{PF}_6)_4$ (purple), $[(\text{Ph}_2\text{phen})_2\text{Ru}(\text{dpp})\text{Ru}(\text{bpy})(\text{dpq})](\text{PF}_6)_4$ (maroon), $[(\text{Ph}_2\text{phen})_2\text{Ru}(\text{dpp})\text{Ru}(\text{bpy})(\text{dpp})\text{PtCl}_2](\text{PF}_6)_4$ (green), and $[(\text{Ph}_2\text{phen})_2\text{Ru}(\text{dpp})\text{Ru}(\text{bpy})(\text{dpq})\text{PtCl}_2](\text{PF}_6)_4$ (blue) measured in deoxygenated RT CH_3CN with $\lambda^{\text{exc}} = 540$ nm.

$$\tau_{\text{model}} = \frac{1}{k_r + k_{nr}} \quad (\text{S4})$$

$$\tau_{\text{tetrametallic}} = \frac{1}{k_r + k_{nr} + k_{et}} \quad (\text{S5})$$

$$\Phi_{3MLCT}^{em(model)} = \Phi_{3MLCT}^{pop(model)} \left(\frac{k_r}{k_r + k_{nr}} \right) \quad (S6)$$

$$\Phi_{3MLCT}^{em(tetrametallic)} = \Phi_{3MLCT}^{pop(tetrametallic)} \left(\frac{k_r}{k_r + k_{nr} + k_{et}} \right) \quad (S7)$$

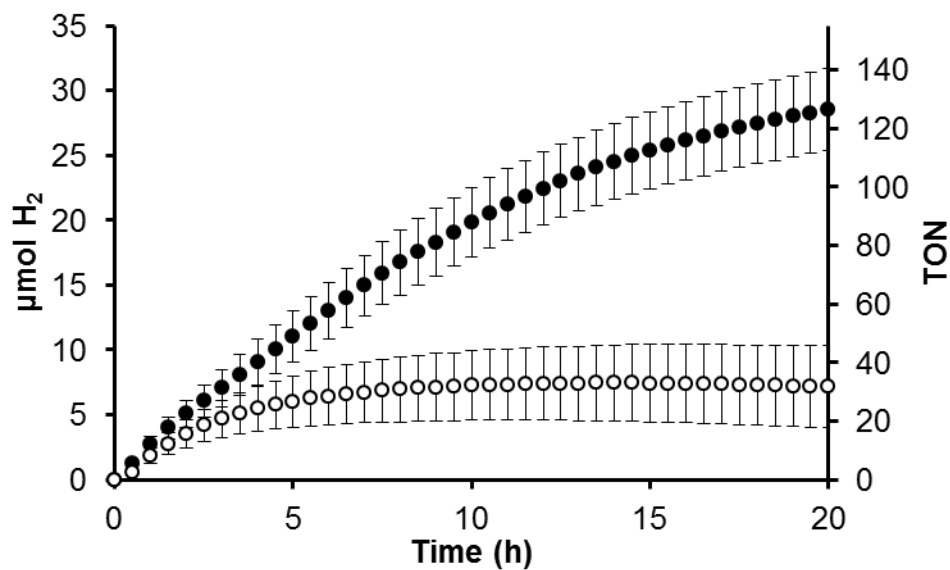


Figure S6. Photocatalytic H_2 production with **RuRudppPt** (black circles) and **$\text{Ru}_2\text{RudppPt}$** (white circles) with $50 \mu\text{M}$ catalyst in spectral grade CH_3CN , $0.62 \text{ M H}_2\text{O}$, 1.5 M DMA , and $110 \mu\text{M}$ $[\text{DMAH}^+][\text{SO}_3\text{CF}_3^-]$. Solutions were irradiated with $\lambda = 470 \pm 10 \text{ nm}$.

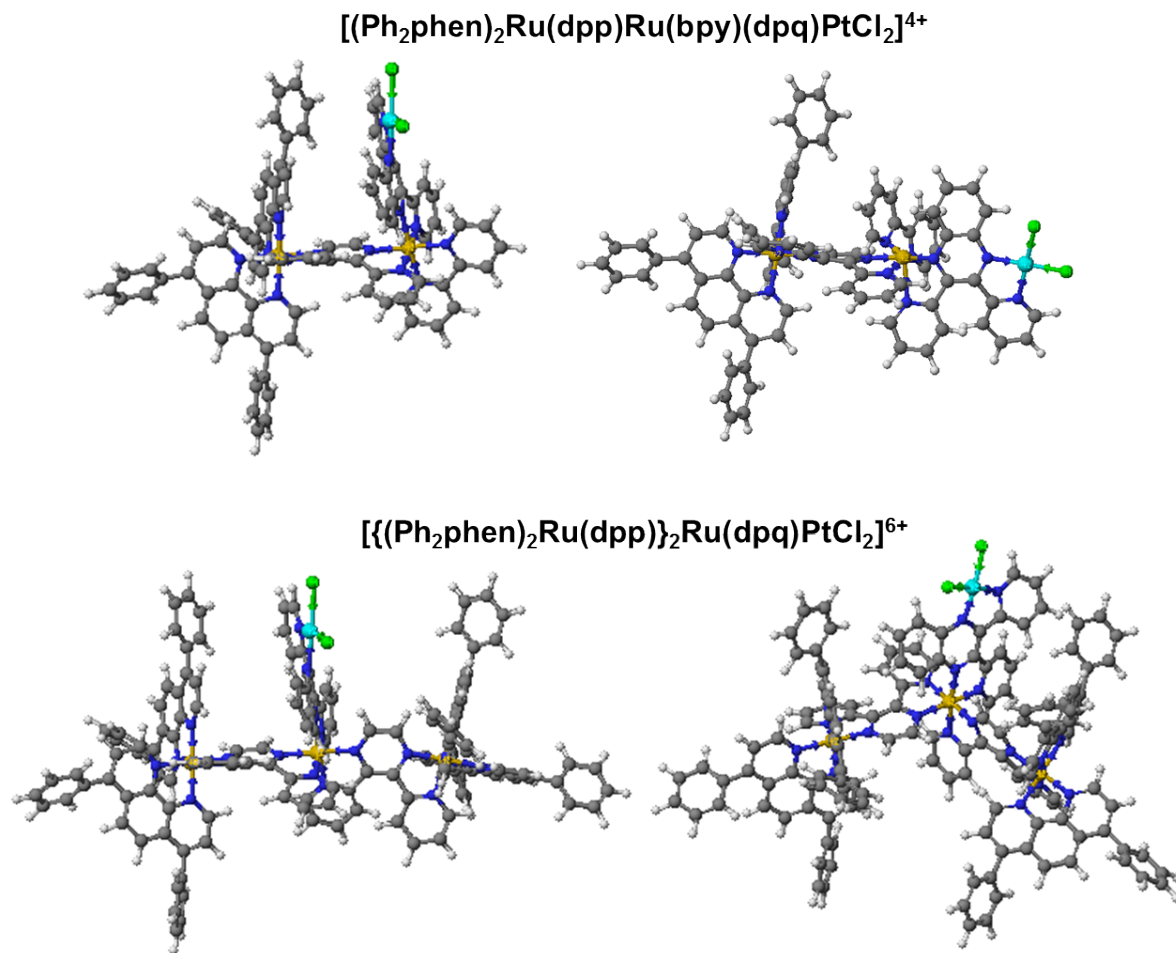


Figure S7. Three dimensional models of $[(\text{Ph}_2\text{phen})_2\text{Ru}(\text{dpp})\text{Ru}(\text{bpy})(\text{dpq})\text{PtCl}_2]^{4+}$ (top) and $[\{(\text{Ph}_2\text{phen})_2\text{Ru}(\text{dpp})\}_2\text{Ru}(\text{dpq})\text{PtCl}_2]^{6+}$ (bottom) showing the impact of isomerism on the sterics around the *cis*-PtCl₂ center. Structures generated and energy minimized using Scigress 7.7.1 molecular modeling software with the MM3 method. Gold = Ru, light blue = Pt, green = Cl, blue = N, gray = C, white = H, Ph₂phen = 4,7-diphenyl-1,10-phenanthroline, bpy = 2,2'-bipyridine, dpp = 2,3-bis(2-pyridyl)pyrazine, dpq = 2,3-bis(2-pyridyl)quinoxaline.

REFERENCES

- [1] a) H. A. Goodwin and F. Lions, *Journal of the American Chemical Society* **1959**, *81*, 6415-6422; b) J. H. Price, A. N. Williamson, R. F. Schramm and B. B. Wayland, *Inorganic Chemistry* **1972**, *11*, 1280-1284; c) M. T. Mongelli and K. J. Brewer, *Inorganic Chemistry Communications* **2006**, *9*, 877-881; d) M. Toyama, K.-I. Inoue, S. Iwamatsu and N. Nagao, *Bulletin of the Chemical Society of Japan* **2006**, *79*, 1525-1534.
- [2] M. Winter in *Sheffield Chemputer*, Vol. **1993-2001**.
- [3] J. V. Caspar, E. M. Kober, B. P. Sullivan and T. J. Meyer, *Journal of the American Chemical Society* **1982**, *104*, 630-632.

[4] J. R. Brown, M. Elvington, M. T. Mongelli, D. F. Zigler and K. J. Brewer, *SPIE Optics+ Photonics*, **2006**, p. 634017.